Evaluating gyro-viscosity in the Kelvin-Helmholtz instability by kinetic simulations

Takayuki Umeda, Natsuki Yamauchi, Yasutaka Wada, and Satoshi Ueno

Articles you may be interested in

Evolution of Kelvin-Helmholtz instability at Venus in the presence of the parallel magnetic field
Phys. Plasmas **22**, 062902 (2015); 10.1063/1.4922753

Evolution of the magnetic field generated by the Kelvin-Helmholtz instability
Phys. Plasmas **21**, 072126 (2014); 10.1063/1.4891340

Nonlinear evolution of the magnetized Kelvin-Helmholtz instability: From fluid to kinetic modeling
Phys. Plasmas **20**, 102118 (2013); 10.1063/1.4826214

2.5D magnetohydrodynamic simulation of the Kelvin-Helmholtz instability around Venus—Comparison of the
influence of gravity and density increase
Phys. Plasmas **19**, 022104 (2012); 10.1063/1.3682039

Kinetic effects on the Kelvin–Helmholtz instability in ion-to-magnetohydrodynamic scale transverse velocity
shear layers: Particle simulations
Phys. Plasmas **17**, 042119 (2010); 10.1063/1.3385445

Evaluating gyro-viscosity in the Kelvin-Helmholtz instability by kinetic simulations

Takayuki Umeda,[a)] Natsuki Yamauchi, Yasutaka Wada, and Satoshi Ueno
Institute for Space-Earth Environmental Research, Nagoya University, Nagoya 464-8601, Japan

In the present paper, the finite-Larmor-radius (gyro-viscous) term [K. V. Roberts and J. B. Taylor, Phys. Rev. Lett. **8**, 197–198 (1962)] is evaluated by using a full kinetic Vlasov simulation result of the Kelvin-Helmholtz instability (KHI). The velocity field and the pressure tensor are calculated from the high-resolution data of the velocity distribution functions obtained by the Vlasov simulation, which are used to approximate the Finite-Larmor-Radius (FLR) term according to Roberts and Taylor [Phys. Rev. Lett. **8**, 197–198 (1962)]. The direct comparison between the pressure tensor and the FLR term shows an agreement. It is also shown that the anisotropic pressure gradient enhanced the linear growth of the KHI when the inner product between the vorticity of the primary velocity shear layer and the magnetic field is negative, which is consistent with the previous FLR-magnetohydrodynamic simulation result. This result suggests that it is not sufficient for reproducing the kinetic simulation result by fluid simulations to include the FLR term (or the pressure tensor) only in the equation of motion for fluid. *Published by AIP Publishing.*
[http://dx.doi.org/10.1063/1.4952632]

Non-magnetohydrodynamic (MHD) effects on various plasma processes are fundamental issues in plasma physics. It is believed that fluid dynamics are dominant at large spatial scales. Kinetic effects come into play a role when the spatial scale is smaller toward gyro radius, inertial length, and Debye length. For studies of multiscale plasma physics, the direct comparison between fluid and kinetic theories/modeling[1] is an essential approach.

Development of the Kelvin-Helmholtz instability (KHI) has been studied by means of self-consistent numerical simulations by many authors. It is known that development of the KHI depends on the orientation of the inner product between the vorticity of the primary velocity shear layer $\mathbf{\Omega} = \nabla \times \mathbf{U}$ and the magnetic field vector $\mathbf{B}$ in kinetic simulations. In magnetospheric plasma physics, this has been discussed in terms of the dawn-dusk asymmetry at Earth's magnetosphere, where $\mathbf{\Omega} \cdot \mathbf{B}$ is positive at the duskside low-latitude magnetospheric boundary but is negative at the dawnside low-latitude magnetospheric boundary.[2] The direction of ion gyro motion and the rotation direction of KH vortices are opposite for $\mathbf{\Omega} \cdot \mathbf{B} > 0$ while these are same for $\mathbf{\Omega} \cdot \mathbf{B} < 0$.

A Finite-Larmor-Radius (FLR) magnetohydrodynamic (MHD) simulation of the KHI has shown that the linear growth rate of unstable KH modes for $\mathbf{\Omega} \cdot \mathbf{B} < 0$ is larger than that for $\mathbf{\Omega} \cdot \mathbf{B} > 0$.[3] In the FLR-MHD simulation, a gyro-viscous/FLR term is added to the equation of motion in the standard MHD equations.[4,5] On the other hand, full kinetic simulations of the KHI have shown that the linear growth rate of unstable KH modes for $\mathbf{\Omega} \cdot \mathbf{B} > 0$ is larger than that for $\mathbf{\Omega} \cdot \mathbf{B} < 0$ independently on the plasma beta and on the density inhomogeneity.[1,2,6,7] Hence, there is a contradiction between the results of the FLR-MHD simulation and the full kinetic simulations.

Let us consider a four-dimensional phase space with two spatial and two velocity dimensions (x, y, v_x, v_y). The MHD equations are derived by taking the zeroth, first, and second moments of the Vlasov equation. The equation of motion (conservation law of momentum) for MHD fluid is given as

$$\frac{\partial}{\partial t}(m_i N \mathbf{U}) + \nabla \cdot (m_i N \mathbf{U}\mathbf{U}) + \nabla \cdot \mathbf{P} = \mathbf{J} \times \mathbf{B}. \quad (1)$$

Note that only the out-of-plane magnetic field B_z component is considered since the out-of-plane current J_z component does not exist in the present coordinate system. According to Roberts and Taylor,[5] the pressure tensor in the two dimensions is approximated as

$$P_{xx} \approx P - \frac{P}{2\omega_c}\left(\frac{\partial U_y}{\partial x} + \frac{\partial U_x}{\partial y}\right), \quad (2)$$

$$P_{yy} \approx P + \frac{P}{2\omega_c}\left(\frac{\partial U_y}{\partial x} + \frac{\partial U_x}{\partial y}\right), \quad (3)$$

$$P_{xy} = P_{yx} \approx \frac{P}{2\omega_c}\left(\frac{\partial U_x}{\partial x} - \frac{\partial U_y}{\partial y}\right), \quad (4)$$

where $P \equiv (P_{xx} + P_{yy})/2$ represents the scalar pressure and $\omega_{cs} \equiv q_s B_z/m_s$ represents the gyro frequency for the species s with sign included to consider the direction of the magnetic field B_z. Then, the FLR-MHD momentum equation is expressed as

$$\frac{\partial}{\partial t}(m_i N \mathbf{U}) + \nabla \cdot (m_i N \mathbf{U}\mathbf{U}) + \nabla P + \nabla \cdot \mathbf{\Pi} = \mathbf{J} \times \mathbf{B}, \quad (5)$$

where $\mathbf{\Pi}$ represents the gyro-viscosity defined as

$$\Pi_{xx} = -\Pi_{yy} = -\frac{P}{2\omega_c}\left(\frac{\partial U_y}{\partial x} + \frac{\partial U_x}{\partial y}\right), \quad (6)$$
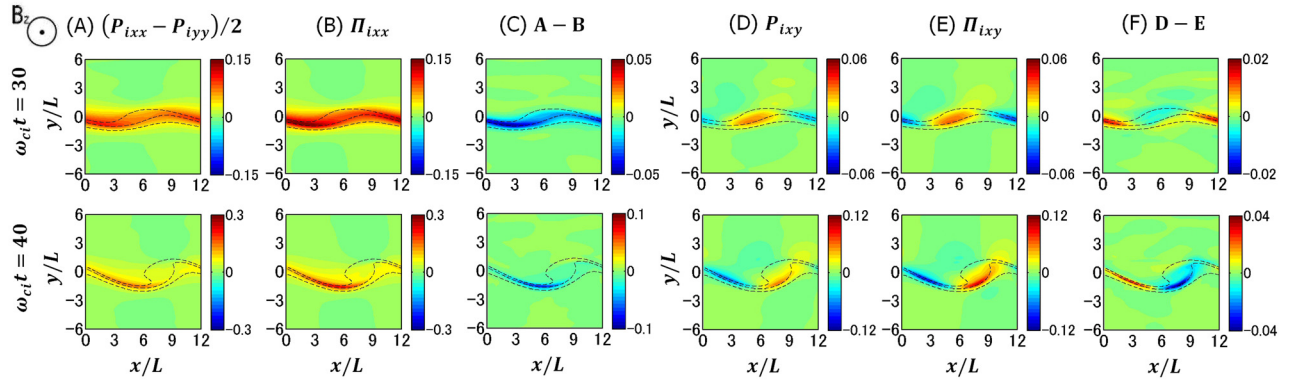
[a)]Email: taka.umeda@nagoya-u.jp

23, 054506-1

FIG. 1. Spatial profiles of $(P_{ixx} - P_{iyy})/2$, Π_{ixx} and their difference, and P_{ixy}, Π_{ixy}, and their difference at $\omega_{ci}t = 30$ and 40 for the run with $\boldsymbol{\Omega} \cdot \boldsymbol{B} > 0$.

$$\Pi_{xy} = \Pi_{yx} = \frac{P}{2\omega_c}\left(\frac{\partial U_x}{\partial x} - \frac{\partial U_y}{\partial y}\right). \qquad (7)$$

It is easy to find that $(P_{xx} - P_{yy})/2 = \Pi_{xx} = -\Pi_{yy}$, and that the gyro-viscosity is used to approximate the pressure tensor.

The purposes of the present study are to evaluate the gyro-viscous terms by using full kinetic simulation data and to discuss reasons for the contradiction between the FLR-MHD and kinetic simulation results. In the present study, we use a full kinetic simulation result obtained by a previous full electromagnetic Vlasov simulation study.[7] The code has two spatial and two velocity dimensions[8] and is based on a non-oscillatory and conservative semi-Lagrangian scheme[9,10] with several improvements.[11–13] The detailed descriptions of the simulation code are given in the references.

The KHI is driven by primary velocity and density shears given by hyperbolic tangent ($U_{yi} = 0.5\Delta U\{1 - \tanh(y/L)\}$ and $N_i = 0.5(N_{low} - N_{high})\tanh(y/L) + 0.5(N_{low} + N_{high})$, where L represents the half thickness of the shear layer). There is a low-density plasma flowing in the $+x$ direction in the lower-part of the simulation domain ($y < 0$) and a high-density plasma at rest in the upper-part of the simulation domain ($y > 0$). The velocity difference and the density ratio are given as $\Delta U = V_A$ and $N_{low}/N_{high} = 0.1$, respectively, where $V_A = B_0/\sqrt{\mu_0 m_i N_{high}}$ is the Alfven velocity. The wavelength of the most linearly unstable KH mode corresponds to $\lambda_{KH} = 12L$, which is much longer than both ion inertial length and ion gyro radius ($\lambda_{KH} \sim 9.3d_i \sim 112.4r_i$ at

$y = 0$). Therefore, the primary KHI is in the MHD regime. Two simulation runs with $\boldsymbol{\Omega} \cdot \boldsymbol{B} > 0$ and $\boldsymbol{\Omega} \cdot \boldsymbol{B} < 0$ were performed to see the effect of the ion gyro motion. Since the vorticity of the initial primary velocity shear is set to be positive in the present simulation runs, the polarity of $\boldsymbol{\Omega} \cdot \boldsymbol{B}$ is controlled by the direction of the out-of-plane magnetic field B_z. The initial density, bulk velocity, temperature of ions, and electrons are determined based on a two-fluid equilibrium. The initial velocity distributions of the ions and electrons are isotropic Maxwellian. Therefore, the initial condition is not a Vlasov equilibrium. See Ref. 7 for the detailed simulation setup and results.

Figures 1 and 2 show the time development of the gyro-viscous terms of ions during the evolution of the KHI for the simulation run with $\boldsymbol{\Omega} \cdot \boldsymbol{B} > 0$ and $\boldsymbol{\Omega} \cdot \boldsymbol{B} < 0$, respectively. The panels (a) show the pressure anisotropy $(P_{ixx} - P_{iyy})/2$ at different times, where the pressure components are calculated from the ion velocity distribution in the Vlasov simulation, the panels (b) show $\Pi_{ixx}(= -\Pi_{iyy})$, which is also calculated by using moment data in the Vlasov simulation based on Eq. (6), and the panels (c) show the difference between (a) and (b). The magnitude of the pressure is normalized by the initial pressure at $y = \pm\infty$. The solid lines show the contour lines of the ion density.

In Fig. 1, both of $(P_{ixx} - P_{iyy})/2$ and Π_{ixx} are enhanced at the velocity shear (density shear) layer at $\omega_{ci}t = 30$ (linear stage) and at a strong density shear layer formed by the vortex formation at $\omega_{ci}t = 40$ (nonlinear stage). Both of $(P_{ixx} - P_{iyy})/2$ and Π_{ixx} are positively polarized at $\omega_{ci}t = 30$ and 40.
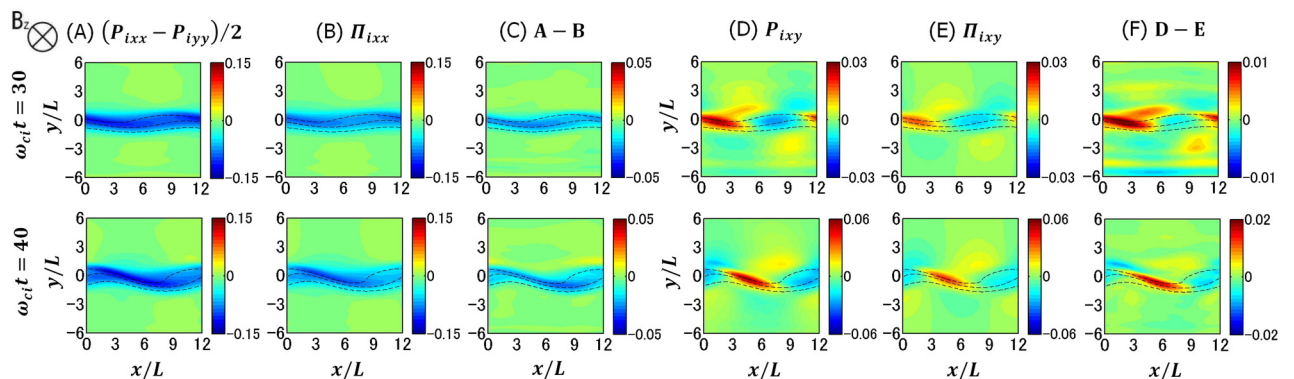

FIG. 2. Spatial profiles of $(P_{ixx} - P_{iyy})/2$, Π_{ixx} and their difference, and P_{ixy}, Π_{ixy}, and their difference at $\omega_{ci}t = 30$ and 40 for the run with $\boldsymbol{\Omega} \cdot \boldsymbol{B} < 0$.
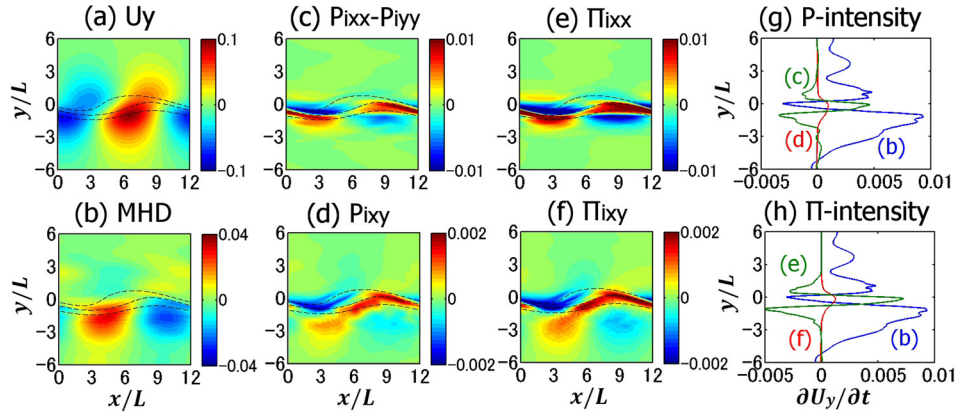
FIG. 3. Contribution of the MHD and non-MHD terms in the linearized equation of motion for fluid (8) at $\omega_{ci}t = 30$ for the run with $\mathbf{\Omega} \cdot \mathbf{B} > 0$. (a) The velocity field U_y, (b) the MHD pressure gradient term in Eq. (8), (c) the $\partial(P_{ixx} - P_{iyy})/\partial y$ term, and (d) the $\partial P_{ixy}/\partial y$ term. (e) The pressure anisotropy $(P_{ixx} - P_{iyy})/2$ in the term (8c) is replaced by Π_{ixx} and (f) the off-diagonal pressure P_{ixy} in the term (8d) is replaced by Π_{ixy}. The spectral intensity of the amplification component of (g) $\mathbf{P}$ and (f) $\mathbf{\Pi}$. The magnitude of the acceleration terms is normalized by $\Delta U^2/L$. The dashed lines in panels (a)–(f) represent the counter lines of the ion density.

The panels (d) show the off-diagonal pressure P_{ixy} at different times, which are calculated from the ion velocity distribution in the Vlasov simulation, the panels (e) show Π_{ixy}, which are calculated based on Eq. (7), and the panels (f) show the difference between (d) and (e). At $\omega_{ci}t = 30$, both of $(P_{ixx} - P_{iyy})/2$ and Π_{ixx} are enhanced at the velocity shear (density shear) layer but vary sinusoidally along the shear layer. At $\omega_{ci}t = 40$, both of $(P_{ixx} - P_{iyy})/2$ and Π_{ixx} are negatively polarized at a strong density shear layer and are positively polarized inside the primary KH vortex.

In contrast to panels (a) and (b) of Fig. 1, both of $(P_{ixx} - P_{iyy})/2$ and Π_{ixx} in Fig. 2 are negatively polarized but have same tendency. Both of P_{ixy} and Π_{ixy} in Fig. 2 also have the opposite polarity to Fig. 1. That is, these are positively polarized at a strong density shear layer and are negatively polarized inside the primary KH vortex. From the comparison among the gyro-viscosity $\mathbf{\Pi}$ and the anisotropic/off-diagonal pressure components $\mathbf{P} - P\mathbf{I}$ of ions, it is shown that these components have similar profiles to each other but have the difference of $\sim 30\%$ in the magnitude.

We next discuss how the anisotropic and off-diagonal pressure components (i.e., $\mathbf{P} - P\mathbf{I}$) affect the linear growth of the KHI. Let us assume that the linear growth of the velocity field U_y is expressed as $U_{y1}(x, y, t) = U_0(y) \exp[ik_x x - i(\omega + i\gamma)t]$. Then, its time derivative is given as $\partial U_{y1}/\partial t = (\gamma - i\omega)U_{y1}$. It is seen that the advection

component has a phase shift by 90° relative to the velocity field U_y, and the amplification component has the same phase as the velocity field U_y. Let us consider the following linearized equation of motion for fluid:

$$\frac{\partial U_{y1}}{\partial t} = -U_{x0}\frac{\partial U_{y1}}{\partial x} \underbrace{- \frac{1}{m_i N}\frac{\partial P_1}{\partial y} - \frac{1}{2\mu_0^2 m_i N}\frac{\partial}{\partial y}(B_{z1}B_{z0})}_{(b)}$$

$$\underbrace{+ \frac{1}{2m_i N}\frac{\partial}{\partial y}(P_{ixx1} - P_{iyy1})}_{(c)} \underbrace{- \frac{1}{m_i N}\frac{\partial P_{ixy1}}{\partial x}}_{(d)}. \quad (8)$$

The first line of Eq. (8) corresponds to the MHD equation of motion, and the second line shows the non-MHD terms. One can understand that the first term (advection term) in the MHD terms does not have the amplification component, and that the MHD pressure gradient terms have both of amplification component and advection component (at the sonic velocity). Note that the scalar pressure P includes both of ion and electron components, while it is found from our Vlasov simulation result that the contribution of electrons in the non-MHD terms, $\partial(P_{exx1} - P_{eyy1})/\partial x$ and $\partial P_{exy1}/\partial x$, is negligible.

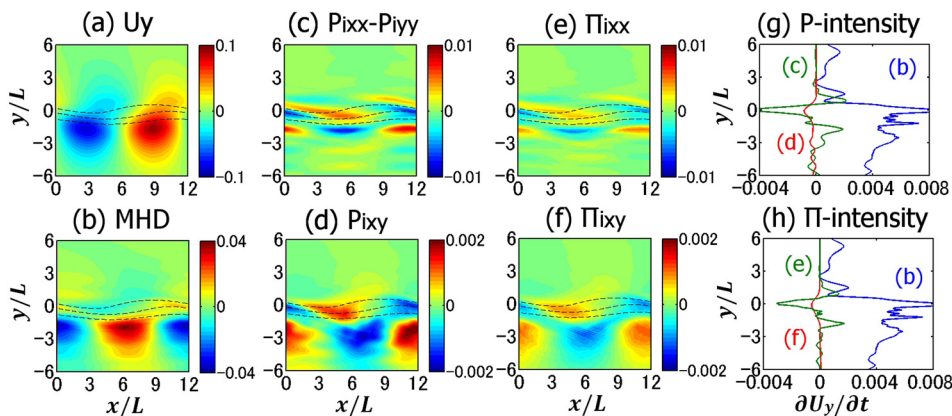Figure 3 shows the contribution of the MHD and non-MHD terms in the linearized equation of motion for fluid (8)

FIG. 4. Contribution of the MHD and non-MHD terms in the linearized equation of motion for fluid (8) at $\omega_{ci}t = 30$ for the run with $\mathbf{\Omega} \cdot \mathbf{B} < 0$ with the same format as Fig. 3.

at $\omega_{ci}t = 30$ for the run with $\boldsymbol{\Omega} \cdot \boldsymbol{B} > 0$. The panels (a)–(d) show the velocity field U_y, the MHD pressure gradient term in Eq. (8), the $\partial(P_{ixx} - P_{iyy})/\partial y$ term, and the $\partial P_{ixy}/\partial y$ term, respectively. In panels (e) and (f), the pressure anisotropy $(P_{ixx} - P_{iyy})/2$ in the term (8c) and the off-diagonal pressure P_{ixy} in the term (8d) are replaced by Π_{ixx} and Π_{ixy}, respectively.

The velocity field U_y has a peak at $y/L \sim -1$. It is seen that the phases of both of MHD and non-MHD terms at $y/L \sim -1$ are almost in the same phase and are shift by $90°$ relative to the velocity field U_y. This suggests that the advection component is dominant in both of MHD and non-MHD terms. Thus, we Fourier-transformed these terms and showed the intensity of the amplification component in panel (g), which has the same phase as the velocity field U_y. It is shown that the off-diagonal pressure P_{ixy} term (d) is small, and that the pressure anisotropy $(P_{ixx} - P_{iyy})/2$ term (c) at $y/L \sim -1$ has the opposite polarity to the MHD pressure gradient term (b). Note that there also exists a strong amplification component at $y/L \sim 0$. However, this component varies in time (oscillates) and does not contribute to the linear growth of the KHI.

Figure 4 shows the contribution of the MHD and non-MHD terms in the linearized equation of motion for fluid (8) at $\omega_{ci}t = 30$ for the run with $\boldsymbol{\Omega} \cdot \boldsymbol{B} < 0$, with the same format as Fig. 3. The velocity field U_y has a peak at $y/L \sim -2$. In contrast to Fig. 3, the pressure anisotropy $(P_{ixx} - P_{iyy})/2$ term (c) at $y/L \sim -2$ has the same polarity as the MHD pressure gradient term (b).

These results suggest that the pressure anisotropy term enhances the linear development of the MHD velocity field in the KHI in the run with $\boldsymbol{\Omega} \cdot \boldsymbol{B} < 0$ rather than in run with $\boldsymbol{\Omega} \cdot \boldsymbol{B} > 0$, which is inconsistent with the previous kinetic simulations.[1,2,6,7] We can also check how the gyro-viscous terms affect the linear development the MHD velocity field in the KHI. As shown in panel (h) of Figs. 3 and 4, the gyro-viscous terms have the same polarity as the pressure tensor terms, which confirms consistency with the previous FLR-MHD simulation.[3]

In summary, it is reconfirmed that the gyro-viscosity is a good (but not perfect) approximation of the pressure tensor. It is also shown that the KHI is accelerated by the pressure tensor term or the gyro-viscous term for $\boldsymbol{\Omega} \cdot \boldsymbol{B} < 0$ and is decelerated for $\boldsymbol{\Omega} \cdot \boldsymbol{B} > 0$, which is consistent with the previous FLR-MHD simulation.[3]

The previous study[1] has shown that the growth rate of the KHI for the Hall-MHD simulation is same for $\boldsymbol{\Omega} \cdot \boldsymbol{B} > 0$ and < 0 with $L = 3d_i$. In the present case, on the other hand, the half thickness of the initial velocity shear layer was set as $L = 0.78 d_i$, in which the Hall effect may not be negligible. Our linear analyses of the MHD and the Hall-MHD equations give the growth rate of the KHI at $k_xL = 0.52$ as $\gamma/\omega_0 = 0.0885$ for MHD, 0.087 for Hall-MHD with $\boldsymbol{\Omega} \cdot \boldsymbol{B} > 0$, and 0.085 for Hall-MHD with $\boldsymbol{\Omega} \cdot \boldsymbol{B} < 0$, where $\omega_0 \equiv \Delta U/L$. The previous Vlasov simulation[7] showed that the growth rate is $\gamma/\omega_0 = 0.078$ for $\boldsymbol{\Omega} \cdot \boldsymbol{B} > 0$ and 0.067 for $\boldsymbol{\Omega} \cdot \boldsymbol{B} < 0$.

Therefore, the influence of the gyro-viscous effect is greater than that of the Hall effect in the present case.

The present result suggests that fluid simulations with the gyro-viscous or the pressure tensor terms *only in the equation of motion* cannot reproduce the result of kinetic simulations. It is expected that the difference between the previous FLR-MHD simulation[3] and the full kinetic simulations[1,2,6,7] comes from the energy equation

$$\frac{\partial}{\partial t}\left(m_i N|\boldsymbol{U}|^2 + 2P\right) = -\nabla \cdot \left(m_i N|\boldsymbol{U}|^2\boldsymbol{U}\right) - 2\nabla \cdot (\boldsymbol{P}\boldsymbol{U})$$
$$-2\nabla \cdot (P\boldsymbol{U}) - \nabla \cdot \boldsymbol{Q} - 2\boldsymbol{E} \cdot \boldsymbol{J}$$
$$= -\nabla \cdot \left(m_i N|\boldsymbol{U}|^2\boldsymbol{U}\right) - 4\nabla \cdot (P\boldsymbol{U}) - 2\boldsymbol{E} \cdot \boldsymbol{J}$$
$$-2\nabla \cdot (\boldsymbol{\Pi}\boldsymbol{U}) - \nabla \cdot \boldsymbol{Q}, \tag{9}$$

where $\boldsymbol{Q} \equiv (Q_{xxx} + Q_{xyy}, Q_{xxy} + Q_{yyy})$ represents a heat flux vector and $\nabla \cdot (\boldsymbol{P}\boldsymbol{U}) = \nabla \cdot (P\boldsymbol{U}) + \nabla \cdot (\boldsymbol{\Pi}\boldsymbol{U})$. The first line of Eq. (9) corresponds to the scalar energy equation for MHD fluids, and the second line corresponds to the non-MHD terms. In the FLR-MHD energy equation, both of the gyro-viscous term and the heat flux term in the second line of Eq. (9) are neglected. To solve the issue on the contradiction between the FLR-MHD simulation and the kinetic simulation, therefore, FLR-MHD simulations including the gyro-viscous terms in the energy conservation law or fluid simulations with the energy tensor equations are necessary, which are left as future studies.

[1]P. Henri, S. S. Cerri, F. Califano, F. Pegoraro, C. Rossi, M. Faganello, O. Sebek, P. M. Travnicek, P. Hellinger, J. T. Frederiksen, A. Nordlund, S. Markidis, R. Keppens, and G. Lapenta, Phys. Plasmas **20**, 102118 (2013).
[2]M. Wilber and R. M. Winglee, J. Geophys. Res. **100**, 1883–1898, doi:10.1029/94JA02488 (1995).
[3]J. D. Huba, Geophys. Res. Lett. **23**, 2907–2910, doi:10.1029/96GL02767 (1996).
[4]W. B. Thompson, Rep. Prog. Phys. **24**, 363–424 (1961).
[5]K. V. Roberts and J. B. Taylor, Phys. Rev. Lett. **8**, 197–198 (1962).
[6]T. K. M. Nakamura, H. Hasegawa, and I. Shinohara, Phys. Plasmas **17**, 042119 (2010).
[7]T. Umeda, S. Ueno, and T. K. M. Nakamura, Plasma Phys. Controlled Fusion **56**, 075006 (2014).
[8]T. Umeda, J. Miwa, Y. Matsumoto, T. K. M. Nakamura, K. Togano, K. Fukazawa, and I. Shinohara, Phys. Plasmas **17**, 052311 (2010).
[9]T. Umeda, Earth, Planets Space **60**, 773–779 (2008).
[10]T. Umeda, Y. Nariyuki, and D. Kariya, Comput. Phys. Commun. **183**, 1094–1100 (2012).
[11]H. Schmitz and R. Grauer, Comput. Phys. Commun. **175**, 86–92 (2006).
[12]T. Umeda, K. Togano, and T. Ogino, Comput. Phys. Commun. **180**, 365–374 (2009).
[13]T. Umeda, K. Fukazawa, Y. Nariyuki, and T. Ogino, IEEE Trans. Plasma Sci. **40**, 1421–1428 (2012).